4

MAGNETIC SCATTERING OF NEUTRONS

The scattering of low-energy neutrons provides an extremely powerful experimental technique for studying the properties of solids. The neutron has a number of special characteristics, on which its utility as a tool for examining magnetic materials depends. Because it is a neutral particle, it can penetrate deeply into most crystals, interacting through its magnetic moment with the electronic moments strongly enough to be measurably scattered, but without disturbing the magnetic system too severely. As a consequence, the great majority of neutrons participate in at most one scattering event, and they sense the properties of the unperturbed crystal. *Thermal neutrons*, with energies of the order of 25 meV, corresponding to wavelengths of the order of 2 Å, match both the interatomic spacings and the energies and momenta of the magnetic excitations, and are generated with adequate intensity by research reactors. *Cold neutrons*, with energies around 5 meV and wavelengths about 4 Å, which are emitted from cooled moderators in reactors, may be even more ideally suited for studying the spatial arrangement and the dynamics of the magnetic moments.

The neutron-scattering cross-section contains precisely that information which is needed to characterize a magnetic material, and to make a stringent comparison with theoretical calculations of its properties. The elastic *Bragg scattering* or *neutron diffraction* provides a systematic procedure for determining the magnetic structure, or the mean values of the magnetic-moment vectors on the different atomic sites. *Inelastic neutron scattering* may be looked upon in three complementary ways. Through conservation of energy and momentum, the scattered neutrons measure the *dispersion relation* of the magnetic excitations. The scattering cross-section is also directly related to the *time-dependent pair-correlation function*, which describes the evolution in space and time of the system of moments. Finally, through the fluctuation–dissipation theorem presented in the last chapter, the cross-section may be expressed in terms of the *generalized susceptibility* of the magnetic crystal, the function describing the dynamics of the moments which is most readily calculated theoretically. No other experimental technique can aspire to providing such detailed microscopic information about magnetic systems.

This chapter does not pretend to be a complete exposition of the theory of magnetic neutron scattering. We shall rather, by elementary

means, derive the magnetic cross-section for unpolarized neutrons in the simple *dipole approximation*, which is normally adequate for scattering by rare earth ions, and will therefore suffice in our further discussion. A neutron interacts with the nuclei in a solid through the nuclear force and, through its magnetic moment, with the magnetic field due to the electrons. In solids with unpaired electrons, the two kinds of scattering mechanism lead to cross-sections of the same order of magnitude. The magnetic field of the electrons may be described by a multipole expansion, and the first term in this series, the dipole term, leads to the dominating contribution to the cross-section at small scattering vectors. We use this approximation in a derivation from first principles of a general expression for the *differential cross-section* (Trammel 1953), which we then separate into *elastic* and *inelastic* components. Using linear response theory, we derive the different forms which the inelastic part may exhibit, and illustrate some of the results by means of the Heisenberg ferromagnet. A detailed treatment of both the nuclear and magnetic scattering of neutrons may be found in Marshall and Lovesey (1971), and Lovesey (1984), while a brief review of some of the salient features of magnetic neutron scattering and its application to physical problems has been given by Mackintosh (1983).

4.1 The differential cross-section in the dipole approximation

A neutron-scattering experiment is performed by allowing a collimated beam of monochromatic (monoenergetic) neutrons to impinge upon a sample, and then measuring the energy distribution of neutrons scattered in different directions. As illustrated in Fig. 4.1, a uniform ensemble of neutrons in the initial state $|\mathbf{k}\mathbf{s}_n>$ is created, typically by utilizing Bragg-reflection in a large single-crystal monochromator, plus suitable shielding by collimators. We may write the state vector for this initial plane-wave state

$$|\mathbf{k}\mathbf{s}_n> = V^{-1/2}\exp(i\mathbf{k}\cdot\mathbf{r}_n)\,|\mathbf{s}_n>\,,$$

representing free neutrons with an energy $(\hbar k)^2/2M$ and a flux $\mathbf{j}(\mathbf{k}\mathbf{s}_n) = V^{-1}\hbar\mathbf{k}/M$. When passing through the target, the probability per unit time that a neutron makes a transition from its initial state to the state $|\mathbf{k}'\mathbf{s}'_n>$ is determined by *Fermi's Golden Rule*:

$$W(\mathbf{k}\mathbf{s}_n, \mathbf{k}'\mathbf{s}'_n) = \frac{2\pi}{\hbar}\sum_{if} P_i\,|<\mathbf{k}\mathbf{s}_n; i\,|\,\mathcal{H}_{\rm int}\,|\mathbf{k}'\mathbf{s}'_n; f>|^2\,\delta(\hbar\omega + E_i - E_f). \tag{4.1.1}$$

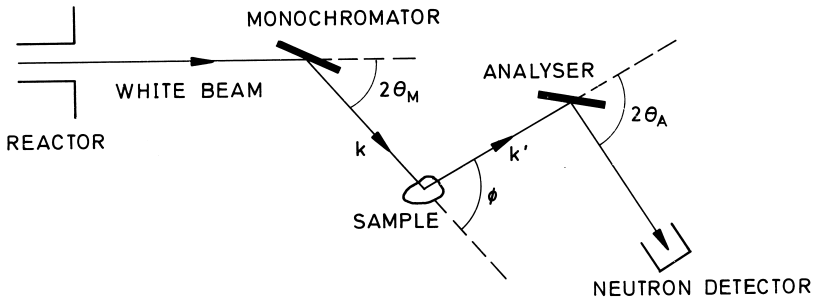

Fig. 4.1. The principle of a neutron-scattering experiment, carried out on a *triple-axis spectrometer*. An incident beam of neutrons, with well-defined momenta, is selected from the continuous reactor spectrum by the monochromator crystal, and scattered from the sample. The intensity of the scattered beam of neutrons, with generally different momenta defined by the analyser crystal, is measured by the detector. The scattered intensity, proportional to the scattering cross-section, is thus determined as a function of the energy transfer $\hbar\omega$ and the momentum transfer $\hbar\boldsymbol{\kappa}$ to the sample, whose orientation relative to $\boldsymbol{\kappa}$ can be varied by rotating the sample table.

$\mathcal{H}_{\rm int}$ is the Hamiltonian describing the interaction between the neutrons and the sample, and the sum extends over all possible scattering processes. It comprises a summation over all possible final states $|f>$ of the sample, and an average over all initial states $|i>$, which occur with the probability P_i. Energy conservation requires that the energy difference between the final and initial states of the sample, $E_f - E_i$, must be equal to the energy transferred from the neutron to it:

$$\hbar\omega = \frac{(\hbar k)^2}{2M} - \frac{(\hbar k')^2}{2M}. \tag{4.1.2}$$

The linear momentum transferred to the sample is $\hbar\boldsymbol{\kappa} = \hbar\mathbf{k} - \hbar\mathbf{k}'$, where $\boldsymbol{\kappa}$ is the *scattering vector*,

$$\boldsymbol{\kappa} = \mathbf{k} - \mathbf{k}'. \tag{4.1.3}$$

The information about the sample is obtained by measuring the scattered intensity as a function of the natural variables of the experiment, the *energy transfer* $\hbar\omega$ and the *momentum transfer* $\hbar\boldsymbol{\kappa}$.

The scattered neutrons with momenta lying in a narrow range around $\hbar\mathbf{k}'$ are counted by placing a detector in a direction along $\mathbf{k}'$, subtending a small element of solid angle $d\Omega$. The value of k', or the final

neutron energy, is determined by again making use of Bragg-reflection in a single-crystal analyser, so that only neutrons with energies in a small interval dE around $(\hbar k')^2/2M$ strike the counter. The number of neutrons in this range, corresponding to a state vector $|\mathbf{k}'\mathbf{s}'_n>$ for the scattered neutrons, is

$$\delta N = V(2\pi)^{-3}(k')^2 dk' d\Omega = V(2\pi)^{-3}(Mk'/\hbar^2) dE d\Omega.$$

The number of neutrons arriving at the counter per unit time and per incident neutron is proportional to the scattering area $d\sigma = |\mathbf{j}(\mathbf{k}\mathbf{s}_n)|^{-1} \times W(\mathbf{k}\mathbf{s}_n, \mathbf{k}'\mathbf{s}'_n)\delta N$, or to the *differential scattering cross-section*

$$\frac{d^2\sigma}{dEd\Omega} = \frac{k'}{k}\left(\frac{M}{2\pi\hbar^2}\right)^2 \sum_{if} P_i \,|<\mathbf{s}_n; i\,|\,\mathcal{H}_{\rm int}(\boldsymbol{\kappa})\,|\,\mathbf{s}'_n; f>|^2\, \delta(\hbar\omega + E_i - E_f), \tag{4.1.4a}$$

where

$$\mathcal{H}_{\rm int}(\boldsymbol{\kappa}) = \int \mathcal{H}_{\rm int}\, e^{-i\boldsymbol{\kappa}\cdot\mathbf{r}_n} d\mathbf{r}_n. \tag{4.1.4b}$$

This result of time-dependent perturbation theory, in the first Born approximation, is accurate because of the very weak interaction between the neutrons and the constituents of the sample.

In order to proceed further, it is necessary to specify the interaction Hamiltonian $\mathcal{H}_{\rm int}$. The magnetic moment of the neutron is

$$\boldsymbol{\mu}_n = -g_n \mu_N \mathbf{s}_n \qquad ; \quad g_n = 3.827 \qquad ; \quad \mu_N = \frac{m}{M}\mu_B = \frac{e\hbar}{2Mc},$$

with $s_n = \frac{1}{2}$. In this chapter, in the interest of conformity with the rest of the literature, we do not reverse the signs of the electronic angular-momentum vectors, which are therefore antiparallel to the corresponding magnetic moments, as is also the case for the neutron.

This magnetic dipole moment at $\mathbf{r}_n$ gives rise to a vector potential, at the position $\mathbf{r}_e$,

$$\mathbf{A}_n(\mathbf{r}_e, \mathbf{r}_n) = \mathbf{A}_n(\mathbf{r} = \mathbf{r}_e - \mathbf{r}_n) = \boldsymbol{\mu}_n \times \mathbf{r}/r^3,$$

with $r = |\mathbf{r}|$. The magnetic-interaction Hamiltonian for a neutron at $\mathbf{r}_n$ with a single electron of charge $-e$, with coordinate $\mathbf{r}_e$, momentum $\mathbf{p}$, and spin $\mathbf{s}$ is

$$\begin{aligned}\mathcal{H}_{\rm int}(\mathbf{r}_e, \mathbf{r}_n) &= \frac{1}{2m}\Big(\mathbf{p} + \frac{e}{c}(\mathbf{A}_n + \mathbf{A}_e)\Big)^2 - \frac{1}{2m}\Big(\mathbf{p} + \frac{e}{c}\mathbf{A}_e\Big)^2 + 2\mu_B \mathbf{s}\cdot\mathbf{B}_n \\ &= 2\mu_B\Big(\frac{1}{\hbar}\mathbf{A}_n \cdot \mathbf{p}' + \mathbf{s}\cdot(\nabla \times \mathbf{A}_n)\Big),\end{aligned} \tag{4.1.5}$$

neglecting the diamagnetic term of second order in μ_N. $\mathbf{A}_e$ denotes the additional contribution to the total vector potential from the surrounding electrons, or an external magnetic field. The prime on $\mathbf{p}$ only plays a role if $\mathbf{A}_e$ is non-zero, in which case $\mathbf{p}' = \mathbf{p} + \frac{e}{c}\mathbf{A}_e$. We note that $\mathbf{A}_n$ commutes with $\mathbf{p}'$, because $\nabla_e \cdot \mathbf{A}_n = \nabla \cdot \mathbf{A}_n$ and

$$\nabla \cdot \mathbf{A}_n(\mathbf{r}) = \nabla \cdot \{-\boldsymbol{\mu}_n \times \nabla(\tfrac{1}{r})\} = \boldsymbol{\mu}_n \cdot \nabla \times \nabla(\tfrac{1}{r}) = 0,$$

recalling that $\mathbf{r}/r^3 = -\nabla(\frac{1}{r})$.

The Fourier transform of $\mathbf{A}_n$ with respect to the neutron coordinate, defining $\mathbf{x} = \mathbf{r}_n - \mathbf{r}_e$, is

$$\begin{aligned}\int \mathbf{A}_n(\mathbf{r}_e - \mathbf{r}_n)\, e^{-i\boldsymbol{\kappa}\cdot\mathbf{r}_n} d\mathbf{r}_n &= e^{-i\boldsymbol{\kappa}\cdot\mathbf{r}_e} \int \mathbf{A}_n(-\mathbf{x})\, e^{-i\boldsymbol{\kappa}\cdot\mathbf{x}} d\mathbf{x} \\ &= -e^{-i\boldsymbol{\kappa}\cdot\mathbf{r}_e} \int (\boldsymbol{\mu}_n \times \mathbf{x})\, x^{-3} e^{-i\boldsymbol{\kappa}\cdot\mathbf{x}} d\mathbf{x} = -e^{-i\boldsymbol{\kappa}\cdot\mathbf{r}_e}\, \frac{4\pi}{i\kappa}\, \boldsymbol{\mu}_n \times \hat{\boldsymbol{\kappa}},\end{aligned}$$

where $\hat{\boldsymbol{\kappa}}$ is a unit vector along $\boldsymbol{\kappa}$ (the integration is performed straightforwardly in spherical coordinates). Applying Green's theorem and assuming V to be a sphere of radius r,

$$\int \nabla \times \left(e^{-i\boldsymbol{\kappa}\cdot\mathbf{x}} \mathbf{A}_n(\mathbf{x})\right) d\mathbf{x} \propto (\kappa r)^{-1} \to 0 \quad \text{for} \quad r \to \infty,$$

from which we deduce

$$\begin{aligned}\int \left(\nabla \times \mathbf{A}_n(\mathbf{x})\right) e^{-i\boldsymbol{\kappa}\cdot\mathbf{x}} d\mathbf{x} &= -\int \left(\nabla\, e^{-i\boldsymbol{\kappa}\cdot\mathbf{x}}\right) \times \mathbf{A}_n(\mathbf{x}) d\mathbf{x} \\ &= i\boldsymbol{\kappa} \times \int e^{-i\boldsymbol{\kappa}\cdot\mathbf{x}} \mathbf{A}_n(\mathbf{x}) d\mathbf{x} = 4\pi \hat{\boldsymbol{\kappa}} \times \boldsymbol{\mu}_n \times \hat{\boldsymbol{\kappa}}\end{aligned}$$

(we note that $\nabla \times \mathbf{A}_n(\mathbf{r}) = \nabla_{(\mathbf{x})} \times \mathbf{A}_n(\mathbf{x})$). From these results, we obtain

$$\begin{aligned}\mathcal{H}_{\text{int}}(\boldsymbol{\kappa}) &= \int \mathcal{H}_{\text{int}}(\mathbf{r}_e, \mathbf{r}_n) e^{-i\boldsymbol{\kappa}\cdot\mathbf{r}_n} d\mathbf{r}_n \\ &= 2\mu_B\, e^{-i\boldsymbol{\kappa}\cdot\mathbf{r}_e}\, 4\pi \left(\frac{i}{\hbar\kappa} \boldsymbol{\mu}_n \times \hat{\boldsymbol{\kappa}} \cdot \mathbf{p}' + \mathbf{s} \cdot (\hat{\boldsymbol{\kappa}} \times \boldsymbol{\mu}_n \times \hat{\boldsymbol{\kappa}})\right),\end{aligned}$$

or

$$\mathcal{H}_{\text{int}}(\boldsymbol{\kappa}) = 8\pi\mu_B\, \boldsymbol{\mu}_n \cdot \left(\frac{i}{\hbar\kappa} \hat{\boldsymbol{\kappa}} \times \mathbf{p}' + \hat{\boldsymbol{\kappa}} \times \mathbf{s} \times \hat{\boldsymbol{\kappa}}\right) e^{-i\boldsymbol{\kappa}\cdot\mathbf{r}_e}. \tag{4.1.6}$$

$\hat{\boldsymbol{\kappa}} \times \mathbf{p}'$ commutes with $\boldsymbol{\kappa} \cdot \mathbf{r}_e$ and therefore also with $\exp(-i\boldsymbol{\kappa} \cdot \mathbf{r}_e)$, and we have made use of the identity $\hat{\boldsymbol{\kappa}} \times \mathbf{a} \times \hat{\boldsymbol{\kappa}} = \mathbf{a} - (\hat{\boldsymbol{\kappa}} \cdot \mathbf{a})\hat{\boldsymbol{\kappa}}$.

For discussing the rare earths, we may restrict ourselves to the case of electrons localized around the lattice sites in a crystal. Further, we define $\mathbf{r}_e = \widetilde{\mathbf{R}}_j + \mathbf{r}$, with $\mathbf{r}$ now being the relative position of the electron belonging to the jth atom at the position $\widetilde{\mathbf{R}}_j$. Equation (4.1.6) may then be written

$$\mathcal{H}_{\rm int}(\boldsymbol{\kappa}) = 8\pi\mu_B\,\boldsymbol{\mu}_n \cdot (\mathbf{Q}_p + \mathbf{Q}_s)\, e^{-i\boldsymbol{\kappa}\cdot\widetilde{\mathbf{R}}_j}, \tag{4.1.7a}$$

introducing

$$\mathbf{Q}_p = \frac{i}{\hbar\kappa}\,\hat{\boldsymbol{\kappa}} \times \mathbf{p}'\, e^{-i\boldsymbol{\kappa}\cdot\mathbf{r}} \qquad ; \qquad \mathbf{Q}_s = \hat{\boldsymbol{\kappa}} \times \mathbf{s} \times \hat{\boldsymbol{\kappa}}\, e^{-i\boldsymbol{\kappa}\cdot\mathbf{r}}. \tag{4.1.7b}$$

In order to calculate the matrix element $< i\,|\,\mathbf{Q}_{p,s}\,|\,f >$, the factor $\exp(-i\boldsymbol{\kappa}\cdot\mathbf{r})$ is expanded in spherical Bessel functions $j_n(\rho)$, and with $\rho = \kappa r$ and $\cos\theta = \boldsymbol{\kappa}\cdot\mathbf{r}/\rho$,

$$\begin{aligned} e^{-i\boldsymbol{\kappa}\cdot\mathbf{r}} &= \sum_{n=0}^{\infty}(2n+1)\,(-i)^n\, j_n(\rho) P_n(\cos\theta) \\ &\simeq j_0(\rho) - 3i\, j_1(\rho)\cos\theta = j_0(\rho) - i\boldsymbol{\kappa}\cdot\mathbf{r}\{j_0(\rho) + j_2(\rho)\}, \end{aligned} \tag{4.1.8}$$

using $j_n(\rho) = \rho\{j_{n-1}(\rho) + j_{n+1}(\rho)\}/(2n+1)$. The truncation of the series is valid for small values of ρ, where

$$j_n(\rho) = (\rho^n/(2n+1)!!)\{1 - \rho^2/(4n+6) + \cdots\}.$$

We note that, although $\boldsymbol{\kappa}\times\mathbf{p}'$ commutes with $\exp(-i\boldsymbol{\kappa}\cdot\mathbf{r})$, it does not commute with the individual terms in (4.1.8). Introducing this expansion in the expression for $\mathbf{Q}_p$, we find

$$\mathbf{Q}_p = \hat{\boldsymbol{\kappa}} \times \Big(\frac{i}{\hbar\kappa} j_0(\rho)\mathbf{p}' + \frac{1}{\hbar}\{j_0(\rho) + j_2(\rho)\}(\hat{\boldsymbol{\kappa}}\cdot\mathbf{r})\mathbf{p}' + \cdots\Big),$$

which can be rearranged to read

$$\mathbf{Q}_p = \tfrac{1}{2}\{j_0(\rho) + j_2(\rho)\}\,\hat{\boldsymbol{\kappa}} \times \mathbf{l}' \times \hat{\boldsymbol{\kappa}} + \mathbf{Q}'_p. \tag{4.1.9a}$$

We have defined

$$\mathbf{Q}'_p = \hat{\boldsymbol{\kappa}} \times \Big(\frac{i}{\hbar\kappa} j_0(\rho)\mathbf{p}' + \frac{1}{2\hbar}\{j_0(\rho) + j_2(\rho)\}\{(\hat{\boldsymbol{\kappa}}\cdot\mathbf{r})\mathbf{p}' + (\hat{\boldsymbol{\kappa}}\cdot\mathbf{p}')\mathbf{r}\} + \cdots\Big), \tag{4.1.9b}$$

where the orbital momentum $\hbar\mathbf{l} = \mathbf{r}\times\mathbf{p}$ and $\hbar\mathbf{l}' = \hbar\mathbf{l} + \frac{e}{c}\,\mathbf{r}\times\mathbf{A}_e$, and used

$$\hat{\boldsymbol{\kappa}} \times \hbar\mathbf{l}' \times \hat{\boldsymbol{\kappa}} = -\hat{\boldsymbol{\kappa}} \times \{\hat{\boldsymbol{\kappa}} \times (\mathbf{r}\times\mathbf{p}')\} = \hat{\boldsymbol{\kappa}} \times \{(\hat{\boldsymbol{\kappa}}\cdot\mathbf{r})\mathbf{p}' - (\hat{\boldsymbol{\kappa}}\cdot\mathbf{p}')\mathbf{r}\},$$

where $[\,\mathbf{l}'\,,\, j_n(\rho)\,] = \mathbf{0}$ and $[\,\hat{\boldsymbol{\kappa}}\times\mathbf{r}\,,\,\hat{\boldsymbol{\kappa}}\cdot\mathbf{p}'\,] = \mathbf{0}$.

If $\mathcal{H}$ is defined to be the Hamiltonian for the electron, then

$$\mathbf{p}' = \mathbf{p} + \frac{e}{c}\mathbf{A}_e = m\, d\mathbf{r}/dt = m\frac{i}{\hbar}[\,\mathcal{H}\,,\,\mathbf{r}\,],$$

and $\mathbf{Q}'_p$ may be written

$$\mathbf{Q}'_p = \frac{m}{\hbar^2\kappa}\,\hat{\boldsymbol{\kappa}} \times \Big(-j_0(\rho)\,[\,\mathcal{H}\,,\,\mathbf{r}\,] + \frac{i\kappa}{2}\{j_0(\rho) + j_2(\rho)\}\,[\,\mathcal{H}\,,\,(\hat{\boldsymbol{\kappa}}\cdot\mathbf{r})\mathbf{r}\,] + \cdots\Big). \tag{4.1.10}$$

Considering an arbitrary operator $\hat{A}$, we have

$$<i\,|\,[\,\mathcal{H}\,,\,\hat{A}\,]\,|\,f> = <i\,|\,\mathcal{H}\hat{A} - \hat{A}\mathcal{H}\,|\,f> = (E_i - E_f)\,<i\,|\,\hat{A}\,|\,f>,$$

which implies that $\mathbf{Q}'_p$ does not contribute to the cross-section (4.1.4) in the limit $\boldsymbol{\kappa} \to \mathbf{0}$. In this limit, $j_n(0) = \delta_{n0}$ and, utilizing the energy δ-function in (4.1.4), the contribution to the cross section due to $\mathbf{Q}'_p$ is seen to be proportional to

$$\left|\frac{m}{\hbar^2\kappa}\,\hbar\omega\,\hat{\boldsymbol{\kappa}} \times <i\,|\,\mathbf{r}\,|\,f>\right|^2 \to 0 \quad \text{for} \quad \kappa \to 0,$$

since $|\hbar\omega| \le (\hbar\kappa)^2/2M$. Introducing the vector operator $\mathbf{K}(\boldsymbol{\kappa})$, defined so that

$$<i\,|\,\hat{\boldsymbol{\kappa}} \times \mathbf{K} \times \hat{\boldsymbol{\kappa}}\,|\,f> = <i\,|\,\mathbf{Q}_p + \mathbf{Q}_s\,|\,f>, \tag{4.1.11}$$

we find, neglecting $\mathbf{Q}'_p$ in the limit $\kappa \to 0$,

$$2\mu_B\mathbf{K}(\mathbf{0}) = \mu_B\,\Big(\mathbf{l} + \frac{e}{\hbar c}\mathbf{r} \times \mathbf{A}_e + 2\mathbf{s}\Big) \equiv -\boldsymbol{\mu}_e, \tag{4.1.12a}$$

or

$$\mathcal{H}_{\text{int}}(\mathbf{0}) = -4\pi\,\boldsymbol{\mu}_n \cdot (\hat{\boldsymbol{\kappa}} \times \boldsymbol{\mu}_e \times \hat{\boldsymbol{\kappa}}), \tag{4.1.12b}$$

implying that the magnetic cross-section (4.1.4), in the limit where the scattering vector approaches zero, is determined by the magnetic dipole moment $\boldsymbol{\mu}_e$ of the electron. In the treatment given above, we have included the diamagnetic contribution to $\boldsymbol{\mu}_e$, induced by external fields $\propto \mathbf{A}_e$. This term may however normally be neglected, as we shall do from now on.

At non-zero κ, we cannot employ directly the above procedure for obtaining an upper bound on the $\mathbf{Q}'_p$ matrix-element, because $j_n(\rho)$ does not commute with $\mathcal{H}$. However, if we restrict ourselves to scattering processes in which the l quantum number is conserved, the matrix element of the first term in (4.1.10) vanishes identically, because $j_0(\rho)$ and $\mathcal{H}$

are both diagonal with respect to l, whereas $\mathbf{r}$ has no diagonal elements (cf. the electric-dipole selection rule $\Delta l = \pm 1$). In the second term of (4.1.10) we can, to leading order, replace $\mathcal{H}$ by the kinetic-energy operator and, if we also make the assumption $\Delta l = 0$, this term transforms like a second-rank tensor and so is quadrupolar. Symmetrizing $\mathbf{Q}'_p$ with respect to the expansion in spherical Bessel functions, and taking $(\hat{\boldsymbol{\kappa}}\cdot\hat{\mathbf{r}})\hat{\mathbf{r}}$ outside the commutator, which is allowed because $\Delta l = 0$, we can write the second term in (4.1.10) as

$$(\hat{\boldsymbol{\kappa}} \times \hat{\mathbf{r}})(\hat{\boldsymbol{\kappa}} \cdot \hat{\mathbf{r}})\, Q_r,$$

with $\hat{\mathbf{r}} = \mathbf{r}/r$ and

$$Q_r = Q_r^\dagger = -\frac{i}{8}\Big(\{j_0(\rho) + j_2(\rho)\}[\,\nabla^2\,,\, r^2\,] + [\,\nabla^2\,,\, r^2\,]\{j_0(\rho) + j_2(\rho)\}\Big).$$

Thus the second term is a product of an angular and a radial operator, which are both Hermitian. Our next assumption is that the radial part of the wavefunction, as specified by the principal quantum number $\tilde{n}$, and by l, is the same in the initial and the final state, i.e. that both $\tilde{n}$ and l are unchanged. In this case, $<i\,|\,Q_r\,|\,f> = <\tilde{n}l\,|\,Q_r\,|\,\tilde{n}l>$ vanishes identically, because Q_r is an imaginary Hermitian operator; $Q_r = Q_r^\dagger = -Q_r^*$. If the radial part of the wavefunction is changed in the scattering process, or if $\mathcal{H}$ is not diagonal in l, then the quadrupole moment leads to an imaginary contribution to $\mathbf{K}(\boldsymbol{\kappa})$, and gives a contribution to the cross-section proportional to κ^2. In most cases of interest, however, this term is very small.

The assumption that $|\,i>$ and $|\,f>$ are linear combinations of the states $|\,(\tilde{n}ls)m_l m_s>$, where $(\tilde{n}ls)$ is constant, implies that the two lowest-order terms in the expansion of Q'_p in (4.1.9*b*) or (4.1.10) can be neglected. Furthermore, the radial and angular dependences are then factorized, both in the expansion of the operators and in the wavefunctions, so that the radial part of the matrix elements may be calculated separately. Hence the orbital contribution $\mathbf{K}_p$ to $\mathbf{K}$ is approximately

$$\mathbf{K}_p(\boldsymbol{\kappa}) = \tfrac{1}{2}\,\{\langle j_0(\kappa)\rangle + \langle j_2(\kappa)\rangle\}\,\mathbf{l}, \qquad (4.1.13a)$$

with

$$\langle j_n(\kappa)\rangle = \int_0^\infty r^2 R^2(r) j_n(\kappa r)\,dr \qquad ; \qquad \int_0^\infty r^2 R^2(r)\,dr = 1, \quad (4.1.13b)$$

where $R(r)$ is the normalized radial wavefunction. The assumption that the final and initial states have the same parity implies that only the terms in the expansion (4.1.8) for which n is odd may contribute to $\mathbf{K}_p$. By the same argument, the spin part $\mathbf{K}_s$ of $\mathbf{K}$ only involves the terms

in (4.1.8) with n even. Neglecting the $(n = 2)$-term in $\mathbf{K}_s$, proportional to $\mathbf{s}$ times an orbital quadrupole moment, we have $\mathbf{K}_s(\boldsymbol{\kappa}) \simeq \langle j_0(\kappa)\rangle\, \mathbf{s}$, or

$$\mathbf{K}(\boldsymbol{\kappa}) = \mathbf{K}(\kappa) = \tfrac{1}{2}\langle j_0(\kappa)\rangle(\mathbf{l} + 2\mathbf{s}) + \tfrac{1}{2}\langle j_2(\kappa)\rangle\, \mathbf{l}. \tag{4.1.14}$$

This result for $\mathbf{K}(\boldsymbol{\kappa})$ is the basis of the dipole approximation for the scattering cross-section. Within this approximation, it is straightforwardly generalized to the case of more than one electron per atom, as the contributions are additive, in the sense that $\mathbf{l}$ and $\mathbf{s}$ are replaced by $\mathbf{L} = \sum \mathbf{l}$ and $\mathbf{S} = \sum \mathbf{s}$, and $R^2(r)$ by the normalized distribution for all unpaired electrons belonging to the atom at $\widetilde{\mathbf{R}}_j$.

The orbital contribution is important in the case of rare earth or actinide ions. In transition-metal ions, the orbital momentum is frequently quenched, and $\mathbf{K}_p$ may then be neglected to leading order. In the rare earths, the spin–orbit coupling is strong and only matrix elements within the ground-state multiplet of $\mathbf{J}^2 = (\mathbf{L}+\mathbf{S})^2$ contribute. In this case, as discussed in Section 1.2, $\mathbf{L} + 2\mathbf{S} = g\mathbf{J}$ and $\mathbf{L} = (2 - g)\mathbf{J}$, where g is the Landé factor, and we have

$$\mathbf{K}(\kappa) = \tfrac{1}{2}\langle j_0(\kappa)\rangle(\mathbf{L} + 2\mathbf{S}) + \tfrac{1}{2}\langle j_2(\kappa)\rangle\mathbf{L} = \tfrac{1}{2}gF(\kappa)\mathbf{J}, \tag{4.1.15a}$$

where $F(\kappa)$ is the *form factor*

$$F(\kappa) = \langle j_0(\kappa)\rangle + \frac{1}{g}(2 - g)\langle j_2(\kappa)\rangle, \tag{4.1.15b}$$

defined so that $F(0) = 1$. When the spin–orbit interaction is introduced, the $(n = 2)$-term in the expansion of $\mathbf{K}_s$ gives a contribution to the dipolar part of $\mathbf{K}(\kappa)$ proportional to $\langle j_2(\kappa)\rangle$, but this is an order of magnitude smaller than the orbital term in (4.1.14). A more systematic approach, making extensive use of Racah tensor-algebra, is required to calculate this term and to include the contributions of the higher-rank multipoles produced by the expansion of $\exp(-i\boldsymbol{\kappa}\cdot\mathbf{r})$. This analysis may be found in Marshall and Lovesey (1971), Stassis and Deckman (1975, 1976), and references therein. Within the present approximation, only tensors of *odd* rank give a contribution to $\mathbf{K}$, proportional to $\kappa^{\tau-1}$, where τ is the rank of the tensors (terms with $\tau = 3$ appear already in order κ^2). In contrast to the dipole contributions, the higher-rank tensor couplings give rise to an angular dependence of $\mathbf{K} = \mathbf{K}(\boldsymbol{\kappa})$. The smaller the scattering wavelength $\lambda = 2\pi/\kappa$, the more the neutron senses the details of the spin and current distributions within the atom, but as long as λ is larger than approximately the mean radius $\langle r\rangle$ of the unpaired electrons, only the dipolar scattering is important. For rare earth ions, $\langle r\rangle \approx 0.6\,\text{Å}$, indicating that (4.1.15) is a valid approximation as long as κ is smaller than about $6\,\text{Å}^{-1}$.

Experimental studies of the form factor and the associated moment densities have been reviewed by Sinha (1978). For an accurate interpretation of the data, it is generally necessary to proceed beyond the dipole approximation. In the heavy rare earths, the deduced $4f$ densities are in good agreement with atomic calculations, provided that relativistic effects are included, but the conduction-electron distributions are much less certain. In the light elements, crystal-field effects become important, as observed for example in Pr and Nd by Lebech *et al.* (1979). Of especial interest is Sm, where the opposition of spin and orbital moments leads to a form factor which has its maximum at a non-zero κ, and the conduction-electron polarization seems to be very strong (Koehler and Moon 1972).

Labelling quantities pertaining to the jth atom with the index j, and summing over all the atoms in the sample, we find that the total $\mathcal{H}_{\rm int}(\boldsymbol{\kappa})$ (4.1.7), in the dipole approximation, is given by

$$\mathcal{H}_{\rm int}(\boldsymbol{\kappa}) = 8\pi\mu_B \sum_j \{\tfrac{1}{2} g F(\kappa)\}_j \, e^{-i\boldsymbol{\kappa}\cdot\widetilde{\mathbf{R}}_j} \, \boldsymbol{\mu}_n \cdot (\hat{\boldsymbol{\kappa}} \times \mathbf{J}_j \times \hat{\boldsymbol{\kappa}}).$$

The squared matrix element in (4.1.4) may furthermore be written

$$< \mathbf{s}_n; i \,|\, \mathcal{H}_{\rm int}(\boldsymbol{\kappa}) \,|\, \mathbf{s}'_n; f >< \mathbf{s}'_n; f \,|\, \mathcal{H}_{\rm int}(-\boldsymbol{\kappa}) \,|\, \mathbf{s}_n; i > .$$

We shall only consider the cross-section for unpolarized neutrons, so that we sum over all the spin states $|\,\mathbf{s}'_n>$ of the scattered neutrons, and average over the spin-states $|\,\mathbf{s}_n>$, with the distribution P_s, of the incoming neutrons. With an equal distribution of up and down spins, $P_s = \frac{1}{2}$, and introducing $\mathbf{Q}_j = \hat{\boldsymbol{\kappa}} \times \mathbf{J}_j \times \hat{\boldsymbol{\kappa}}$, we find that the cross-section is proportional to

$$\begin{aligned}
&\sum_{\mathbf{s}_n \mathbf{s}'_n} P_s < \mathbf{s}_n \,|\, \boldsymbol{\mu}_n \cdot \mathbf{Q}_j \,|\, \mathbf{s}'_n >< \mathbf{s}'_n \,|\, \boldsymbol{\mu}_n \cdot \mathbf{Q}_{j'} \,|\, \mathbf{s}_n > \\
&\qquad = \sum_{\mathbf{s}} P_s < \mathbf{s}_n \,|\, (\boldsymbol{\mu}_n \cdot \mathbf{Q}_j)\,(\boldsymbol{\mu}_n \cdot \mathbf{Q}_{j'}) \,|\, \mathbf{s}_n > = \left(\tfrac{1}{2} g_n \mu_N\right)^2 \, \mathbf{Q}_j \cdot \mathbf{Q}_{j'},
\end{aligned}$$

as may readily be shown by using the Pauli-matrix representation, in which $\mathrm{Tr}\{\sigma_\alpha \sigma_\beta\} = 2\,\delta_{\alpha\beta}$. We have further that $\mathbf{Q}_j \cdot \mathbf{Q}_{j'}$ may be written

$$\begin{aligned}
(\hat{\boldsymbol{\kappa}} \times \mathbf{J}_j \times \hat{\boldsymbol{\kappa}}) \cdot (\hat{\boldsymbol{\kappa}} \times \mathbf{J}_{j'} \times \hat{\boldsymbol{\kappa}}) &= (\mathbf{J}_j - \hat{\boldsymbol{\kappa}}(\mathbf{J}_j \cdot \hat{\boldsymbol{\kappa}})) \cdot (\mathbf{J}_{j'} - \hat{\boldsymbol{\kappa}}(\mathbf{J}_{j'} \cdot \hat{\boldsymbol{\kappa}})) \\
&= \mathbf{J}_j \cdot \mathbf{J}_{j'} - (\mathbf{J}_j \cdot \hat{\boldsymbol{\kappa}})\,(\mathbf{J}_{j'} \cdot \hat{\boldsymbol{\kappa}}) = \sum_{\alpha\beta} \left(\delta_{\alpha\beta} - \hat{\kappa}_\alpha \hat{\kappa}_\beta\right) \, J_{j\alpha} \, J_{j'\beta},
\end{aligned}$$

in terms of the Cartesian components. Defining $(\mathbf{J}_\perp)_j$ to be the projection of $\mathbf{J}_j$ on the plane perpendicular to $\boldsymbol{\kappa}$, we have

$$\sum_{\alpha\beta} \left(\delta_{\alpha\beta} - \hat{\kappa}_\alpha \hat{\kappa}_\beta\right) \, J_{j\alpha} \, J_{j'\beta} = (\mathbf{J}_\perp)_j \cdot (\mathbf{J}_\perp)_{j'}.$$

The various factors in these expressions may be combined to give

$$\frac{k'}{k}\left(\frac{M}{2\pi\hbar^2}\,8\pi\mu_B\,\tfrac{1}{2}g_n\mu_N\right)^2=\frac{k'}{k}\left(\frac{\hbar\gamma e^2}{mc^2}\right)^2\qquad;\quad\gamma=\frac{1}{2\hbar}\,g_n.$$

γ is the gyromagnetic ratio of the neutron, and $e^2/mc^2 = 2.82$ fm is the classical electron radius. The differential cross-section, in the dipole approximation, for the scattering of unpolarized neutrons is then finally

$$\frac{d^2\sigma}{dEd\Omega}=\frac{k'}{k}\left(\frac{\hbar\gamma e^2}{mc^2}\right)^2\sum_{\alpha\beta}(\delta_{\alpha\beta}-\hat\kappa_\alpha\hat\kappa_\beta)\sum_{jj'}\{\tfrac{1}{2}gF(\kappa)\}_j\{\tfrac{1}{2}gF(\kappa)\}_{j'}$$
$$\times\sum_{if}P_i<i\,|\,J_{j\alpha}\,e^{-i\boldsymbol{\kappa}\cdot\widetilde{\mathbf{R}}_j}\,|\,f><f\,|\,J_{j'\beta}\,e^{i\boldsymbol{\kappa}\cdot\widetilde{\mathbf{R}}_{j'}}\,|\,i>\delta(\hbar\omega+E_i-E_f),\tag{4.1.16}$$

where the total magnetic cross-section is $4\pi(\hbar\gamma e^2/mc^2)^2 = 3.65$ barns.

4.2 Elastic and inelastic neutron scattering

If the scattering system is assumed to be in thermal equilibrium at temperature T, the average over initial states in (4.1.16) is the same as the thermal average $\langle\cdots\rangle = \mathrm{Tr}\{\rho_0\cdots\}$, where ρ_0 is the density operator defined in eqn (3.1.1). The atom at the position $\widetilde{\mathbf{R}}_j = \mathbf{R}_j + \mathbf{u}_j$ vibrates around its equilibrium position, the lattice point $\mathbf{R}_j$, and we may write

$$\langle e^{-i\boldsymbol{\kappa}\cdot(\widetilde{\mathbf{R}}_j-\widetilde{\mathbf{R}}_{j'})}\rangle=e^{-2W(\boldsymbol{\kappa})}\,e^{-i\boldsymbol{\kappa}\cdot(\mathbf{R}_j-\mathbf{R}_{j'})},$$

where $W(\boldsymbol{\kappa})$ is the *Debye–Waller factor* $\approx \frac{1}{6}\kappa^2\langle u^2\rangle$, discussed in detail by, for example, Marshall and Lovesey (1971). We insert this term in (4.1.16), and thereby neglect contributions from inelastic phonon-scattering processes, the so-called magneto-vibrational part of the magnetic cross-section. The integral representation of the δ-function is

$$\delta(\hbar\omega+E_i-E_f)=\frac{1}{2\pi\hbar}\int_{-\infty}^{\infty}e^{i(\hbar\omega+E_i-E_f)t/\hbar}dt,$$

which allows us to write

$$\sum_{if}P_i<i\,|\,J_{j\alpha}\,|\,f><f\,|\,J_{j'\beta}\,|\,i>\delta(\hbar\omega+E_i-E_f)$$
$$=\sum_{if}\frac{1}{2\pi\hbar}\int_{-\infty}^{\infty}dt\,e^{i\omega t}P_i<i\,|\,e^{i\mathcal{H}t/\hbar}J_{j\alpha}e^{-i\mathcal{H}t/\hbar}\,|\,f><f\,|\,J_{j'\beta}\,|\,i>$$
$$=\frac{1}{2\pi\hbar}\int_{-\infty}^{\infty}dt\,e^{i\omega t}\sum_i P_i<i\,|\,J_{j\alpha}(t)\,J_{j'\beta}(0)\,|\,i>$$
$$=\frac{1}{2\pi\hbar}\int_{-\infty}^{\infty}dt\,e^{i\omega t}\langle J_{j\alpha}(t)\,J_{j'\beta}(0)\rangle,$$

where $J_{j\alpha}(t)$ is the angular-momentum operator in the Heisenberg picture, as in (3.2.1),

$$J_{j\alpha}(t) = e^{i\mathcal{H}t/\hbar}\, J_{j\alpha}\, e^{-i\mathcal{H}t/\hbar}.$$

At thermal equilibrium, the differential cross-section can then be written

$$\frac{d^2\sigma}{dEd\Omega} = \frac{k'}{k}\left(\frac{\hbar\gamma e^2}{mc^2}\right)^2 e^{-2W(\kappa)} \sum_{\alpha\beta}(\delta_{\alpha\beta} - \hat{\kappa}_\alpha\hat{\kappa}_\beta) \sum_{jj'} \{\tfrac{1}{2}gF(\boldsymbol{\kappa})\}_j \{\tfrac{1}{2}gF(-\boldsymbol{\kappa})\}_{j'} \times \frac{1}{2\pi\hbar}\int_{-\infty}^{\infty} dt\, e^{i\omega t} e^{-i\boldsymbol{\kappa}\cdot(\mathbf{R}_j - \mathbf{R}_{j'})} \langle J_{j\alpha}(t)\, J_{j'\beta}(0)\rangle. \tag{4.2.1}$$

If the magnetic atoms are all identical, the form factor may be taken outside the summation and the cross-section reduces to

$$\frac{d^2\sigma}{dEd\Omega} = N\,\frac{k'}{k}\left(\frac{\hbar\gamma e^2}{mc^2}\right)^2 e^{-2W(\kappa)} |\tfrac{1}{2}gF(\boldsymbol{\kappa})|^2 \sum_{\alpha\beta}(\delta_{\alpha\beta} - \hat{\kappa}_\alpha\hat{\kappa}_\beta)\, \mathcal{S}^{\alpha\beta}(\boldsymbol{\kappa},\omega), \tag{4.2.2a}$$

where we have introduced the *Van Hove scattering function* (Van Hove 1954)

$$\mathcal{S}^{\alpha\beta}(\boldsymbol{\kappa},\omega) = \frac{1}{2\pi\hbar}\int_{-\infty}^{\infty} dt\, e^{i\omega t}\frac{1}{N}\sum_{jj'} e^{-i\boldsymbol{\kappa}\cdot(\mathbf{R}_j - \mathbf{R}_{j'})} \langle J_{j\alpha}(t)\, J_{j'\beta}(0)\rangle, \tag{4.2.2b}$$

which is $(2\pi\hbar)^{-1}$ times the Fourier transform, in space and time, of the pair-correlation function $\langle J_{j\alpha}(t)\, J_{j'\beta}(0)\rangle$. If $\langle J_{j\alpha}\rangle\langle J_{j'\beta}\rangle$ is added and subtracted, the scattering function may be written as the sum of a static and a dynamic contribution:

$$\mathcal{S}^{\alpha\beta}(\boldsymbol{\kappa},\omega) = \mathcal{S}^{\alpha\beta}(\boldsymbol{\kappa}) + \mathcal{S}_d^{\alpha\beta}(\boldsymbol{\kappa},\omega), \tag{4.2.3a}$$

where the static or *elastic* component is

$$\mathcal{S}^{\alpha\beta}(\boldsymbol{\kappa}) = \delta(\hbar\omega)\frac{1}{N}\sum_{jj'}\langle J_{j\alpha}\rangle\, \langle J_{j'\beta}\rangle e^{-i\boldsymbol{\kappa}\cdot(\mathbf{R}_j - \mathbf{R}_{j'})} \tag{4.2.3b}$$

and the *inelastic* contribution is

$$\mathcal{S}_d^{\alpha\beta}(\boldsymbol{\kappa},\omega) = \frac{1}{2\pi\hbar} S_{\alpha\beta}(\boldsymbol{\kappa},\omega) = \frac{1}{\pi}\frac{1}{1 - e^{-\beta\hbar\omega}}\,\chi''_{\alpha\beta}(\boldsymbol{\kappa},\omega). \tag{4.2.3c}$$

We have introduced the dynamic correlation function $S_{\alpha\beta}(\boldsymbol{\kappa},\omega)$, defined by eqn (3.2.13), with

$$\hat{\alpha} = N^{-\frac{1}{2}} \sum_j J_{j\alpha} e^{-i\boldsymbol{\kappa}\cdot\mathbf{R}_j} \quad \text{and} \quad \hat{\beta} = N^{-\frac{1}{2}} \sum_{j'} J_{j'\beta} e^{i\boldsymbol{\kappa}\cdot\mathbf{R}_{j'}},$$

and the corresponding susceptibility function $\chi_{\alpha\beta}(\boldsymbol{\kappa},\omega)$, utilizing the relation between the two functions given by the fluctuation–dissipation theorem (3.2.18).

An important consequence of (4.2.2–3) is that the *inelastic scattering of neutrons* is proportional to the correlation function $S_{\alpha\beta}(\boldsymbol{\kappa},\omega)$, which is essentially the Fourier transform of the probability that, if the moment at site j has some specified vector value at time zero, then the moment at site j' has some other specified value at time t. An inelastic neutron-scattering experiment is thus extremely informative about the dynamics of the magnetic system. Poles in the correlation function, or in $\chi_{\alpha\beta}(\boldsymbol{\kappa},\omega)$, are reflected as peaks in the intensity of the scattered neutrons. According to (4.1.2) and (4.1.3), each neutron in such a scattering peak has imparted energy $\hbar\omega$ and momentum $\hbar\boldsymbol{\kappa}$ to the sample, so the peak is interpreted, depending on whether $\hbar\omega$ is positive or negative, as being due to the creation or annihilation of *quasi-particles* or *elementary excitations* in the system, with energy $|\hbar\omega|$ and crystal momentum $\hbar\mathbf{q} = \hbar(\boldsymbol{\kappa} - \boldsymbol{\tau})$, where $\boldsymbol{\tau}$ is a reciprocal lattice vector. A part of the momentum $\hbar\boldsymbol{\tau}$ may be transferred to the crystal as a whole. If the sample is a single crystal, with only one magnetic atom per unit cell, $S_{\alpha\beta}(\boldsymbol{\kappa},\omega) = S_{\alpha\beta}(\mathbf{q} = \boldsymbol{\kappa} - \boldsymbol{\tau},\omega)$, where $\boldsymbol{\tau}$ is normally chosen so that $\mathbf{q}$ lies within the primitive Brillouin zone. The form factor in the scattering amplitude is not however invariant with respect to the addition of a reciprocal lattice vector. This interpretation of the poles in $S_{\alpha\beta}(\mathbf{q},\omega)$ governs the choice of sign in the exponential arguments in both the temporal and the spatial Fourier transforms.

The relation (4.2.3*c*) between the scattering function and the generalized susceptibility implies that the neutron may be considered as a magnetic probe which effectively establishes a frequency- and wavevector-dependent magnetic field in the scattering sample, and detects its response to this field. This is a particularly fruitful way of looking at a neutron scattering experiment because, as shown in Chapter 3, the susceptibility may be calculated from linear response theory, and thus provides a natural bridge between theory and experiment. Using the symmetry relation (3.2.15), which may here be written $\chi^*_{\alpha\beta}(\mathbf{q},z) = \chi_{\alpha\beta}(-\mathbf{q},-z^*)$, it is straightforward to show that $\chi''_{\alpha\beta}(\mathbf{q},\omega)+\chi''_{\beta\alpha}(\mathbf{q},\omega)$ is real and equal to $\mathrm{Im}\big\{\chi_{\alpha\beta}(\mathbf{q},\omega)+\chi_{\beta\alpha}(\mathbf{q},\omega)\big\}$. In addition, the form of the inelastic cross-section, and also the result (3.3.2) for the dissipation rate, impose another analytic condition on the function $\chi''_{\alpha\beta}(\mathbf{q},\omega)+\chi''_{\beta\alpha}(\mathbf{q},\omega)$.

It must be either zero, or positive or negative with ω (such functions are called *herglotz functions*), because a negative value of the cross-section is clearly unphysical.

If the magnetic moments in a Bravais lattice are ordered in a static structure, described by the wave-vector $\mathbf{Q}$, we may write

$$\langle J_{j\alpha}\rangle = \tfrac{1}{2}\left(\langle J_\alpha\rangle\, e^{i\mathbf{Q}\cdot\mathbf{R}_j} + \langle J_\alpha\rangle^* e^{-i\mathbf{Q}\cdot\mathbf{R}_j}\right), \tag{4.2.4}$$

allowing $\langle J_\alpha\rangle$ to be complex in order to account for the phase. The static contribution to the cross-section is then proportional to

$$\sum_{\alpha\beta}(\delta_{\alpha\beta}-\hat\kappa_\alpha\hat\kappa_\beta)\,\mathcal{S}^{\alpha\beta}(\boldsymbol{\kappa}) = \sum_{\alpha\beta}(\delta_{\alpha\beta}-\hat\kappa_\alpha\hat\kappa_\beta)\,\mathrm{Re}\left\{\langle J_\alpha\rangle\langle J_\beta\rangle^*\right\} \times\ \delta(\hbar\omega)\frac{(2\pi)^3}{\upsilon}\sum_{\boldsymbol{\tau}}\tfrac{1}{4}(1+\delta_{Q0})\left\{\delta(\boldsymbol{\tau}+\mathbf{Q}-\boldsymbol{\kappa})+\delta(\boldsymbol{\tau}-\mathbf{Q}-\boldsymbol{\kappa})\right\}, \tag{4.2.5}$$

where δ_{Q0} is equal to 1 in the ferromagnetic case $\mathbf{Q}=\mathbf{0}$, and zero otherwise, and υ is the volume of a unit cell. The magnetic ordering of the system leads to δ-function singularities in momentum space, corresponding to *magnetic Bragg scattering*, whenever the scattering vector is equal to $\pm\mathbf{Q}$ plus a reciprocal lattice vector $\boldsymbol{\tau}$. The static and dynamic contributions from $\mathcal{S}^{\alpha\beta}(\boldsymbol{\kappa})$ and $\mathcal{S}_d^{\alpha\beta}(\boldsymbol{\kappa},\omega)$ to the total integrated scattering intensity may be comparable, but the dynamic contributions, including possibly a quasi-elastic diffusive term, are distributed more or less uniformly throughout reciprocal space. Consequently, the elastic component, determined by $\mathcal{S}^{\alpha\beta}(\boldsymbol{\kappa})$, in which the scattering is condensed into points in reciprocal space, is overwhelmingly the most intense contribution to the cross-section $d\sigma/d\Omega$, obtained from the differential cross-section (4.2.2*a*) by an energy integration:

$$\frac{d\sigma}{d\Omega} \simeq N\left(\frac{\hbar\gamma e^2}{mc^2}\right)^2 e^{-2W(\kappa)}|\tfrac{1}{2}gF(\boldsymbol{\kappa})|^2\sum_{\alpha\beta}(\delta_{\alpha\beta}-\hat\kappa_\alpha\hat\kappa_\beta)\,\mathrm{Re}\left\{\langle J_\alpha\rangle\langle J_\beta\rangle^*\right\} \times\ \frac{(2\pi)^3}{\upsilon}\sum_{\boldsymbol{\tau}}\tfrac{1}{4}(1+\delta_{Q0})\left\{\delta(\boldsymbol{\tau}+\mathbf{Q}-\boldsymbol{\kappa})+\delta(\boldsymbol{\tau}-\mathbf{Q}-\boldsymbol{\kappa})\right\}. \tag{4.2.6}$$

$d\sigma/d\Omega$ is the cross-section measured in *neutron diffraction* experiments, in which all neutrons scattered in the direction of $\mathbf{k}'$ are counted without energy discrimination, i.e. without the analyser crystal in Fig. 4.1. This kind of experiment is more straightforward to perform than one in which, for instance, only elastically scattered neutrons are counted. In the ordered phase, (4.2.6) is a good approximation, except close to a second-order phase transition, where $\langle J_\alpha\rangle$ is small and where *critical fluctuations*

may lead to strong inelastic or quasi-elastic scattering in the vicinity of the magnetic Bragg peaks.

Independently of whether the magnetic system is ordered or not, the total integrated scattering intensity in the Brillouin zone has a definite magnitude, determined by the size of the local moments and the following sum rule:

$$\begin{aligned}\frac{1}{N}\sum_{\mathbf{q}}\sum_{\alpha}\int_{-\infty}^{\infty}\mathcal{S}^{\alpha\alpha}(\mathbf{q},\omega)d(\hbar\omega)&\\ =\frac{1}{N}\sum_{j}\sum_{\alpha}\langle J_{j\alpha}\rangle^2+\frac{1}{N}\sum_{\mathbf{q}}\sum_{\alpha}S_{\alpha\alpha}(\mathbf{q},t=0)&\\ =\frac{1}{N}\sum_{j}\sum_{\alpha}\langle J_{j\alpha}J_{j\alpha}\rangle=J(J+1),&\end{aligned}\tag{4.2.7}$$

and taking into account the relatively slow variation of the other parameters specifying the cross-section. This implies, for instance, that $d\sigma/d\Omega$ is non-zero in the paramagnetic phase, when $\langle J_\alpha\rangle = 0$, but the distribution of the available scattered intensity over all solid angles makes it hard to separate from the background. In this case, much more useful information may be obtained from the differential cross-section measured in an inelastic neutron-scattering experiment.

For a crystal with a basis of p magnetic atoms per unit cell, the ordering of the moments corresponding to (4.2.4) is

$$\langle J_{j_s\alpha}\rangle=\tfrac{1}{2}\left(\langle J_{s\alpha}\rangle\, e^{i\mathbf{Q}\cdot\mathbf{R}_{j_s}}+\langle J_{s\alpha}\rangle^{*}e^{-i\mathbf{Q}\cdot\mathbf{R}_{j_s}}\right),\tag{4.2.8a}$$

where

$$\mathbf{R}_{j_s}=\mathbf{R}_{j_0}+\mathbf{d}_s,\quad\text{with}\quad s=1,2,\cdots,p.\tag{4.2.8b}$$

Here $\mathbf{R}_{j_0}$ specifies the position of the unit cell, and $\mathbf{d}_s$ is the vector determining the equilibrium position of the sth atom in the unit cell. The summation over the atoms in (4.2.2) may be factorized as follows:

$$\begin{aligned}&\sum_{ij}e^{-i\boldsymbol{\kappa}\cdot(\mathbf{R}_i-\mathbf{R}_j)}\\ &\quad=\sum_{i_0j_0}e^{-i\boldsymbol{\kappa}\cdot(\mathbf{R}_{i_0}-\mathbf{R}_{j_0})}\sum_{s=1}^{p}e^{-i\boldsymbol{\kappa}\cdot(\mathbf{R}_{i_s}-\mathbf{R}_{i_0})}\sum_{r=1}^{p}e^{i\boldsymbol{\kappa}\cdot(\mathbf{R}_{j_r}-\mathbf{R}_{j_0})}\\ &\quad=\sum_{i_0j_0}e^{-i\boldsymbol{\kappa}\cdot(\mathbf{R}_{i_0}-\mathbf{R}_{j_0})}\,|F_G(\boldsymbol{\kappa})|^2\qquad;\quad F_G(\boldsymbol{\kappa})=\sum_{s=1}^{p}e^{-i\boldsymbol{\kappa}\cdot\mathbf{d}_s},\end{aligned}$$

where $F_G(\boldsymbol{\kappa})$ is the *geometric structure factor*. The elastic cross-section then becomes

$$\frac{d\sigma}{d\Omega} = N_0 \left(\frac{\hbar\gamma e^2}{mc^2}\right)^2 e^{-2W(\kappa)} |\tfrac{1}{2} g F(\boldsymbol{\kappa})|^2 \sum_{\alpha\beta} (\delta_{\alpha\beta} - \hat{\kappa}_\alpha \hat{\kappa}_\beta) \, |\langle J_\alpha \rangle \langle J_\beta \rangle| \times$$
$$\frac{(2\pi)^3}{v} \sum_{\boldsymbol{\tau}} \tfrac{1}{4}(1 + \delta_{Q0}) \mathrm{Re}\big\{F_\alpha(\boldsymbol{\tau}) F^*_\beta(\boldsymbol{\tau})\big\} \{\delta(\boldsymbol{\tau} + \mathbf{Q} - \boldsymbol{\kappa}) + \delta(\boldsymbol{\tau} - \mathbf{Q} - \boldsymbol{\kappa})\} \tag{4.2.9a}$$

where N_0 is the number of unit cells, and the *structure factor* is

$$F_\alpha(\boldsymbol{\tau}) = |\langle J_\alpha \rangle|^{-1} \sum_{s=1}^{r} \langle J_{s\alpha} \rangle \, e^{-i\boldsymbol{\tau}\cdot\mathbf{d}_s}. \tag{4.2.9b}$$

As an example, we return to the Heisenberg ferromagnet discussed in Chapter 3. The magnitude of the ordered moments and their direction relative to the crystal lattice, defined to be the z-axis, may be determined by neutron diffraction, since

$$\frac{d\sigma}{d\Omega} = N \left(\frac{\hbar\gamma e^2}{mc^2}\right)^2 e^{-2W(\kappa)} |\tfrac{1}{2} g F(\boldsymbol{\kappa})|^2 (1 - \hat{\kappa}_z^2) \, \langle S_z \rangle^2 \, \frac{(2\pi)^3}{v} \sum_{\boldsymbol{\tau}} \delta(\boldsymbol{\tau} - \boldsymbol{\kappa}). \tag{4.2.10}$$

The Bragg-peak intensity is thus proportional to the square of the ordered moment and to $\sin^2\theta$, where θ is the angle between the magnetization and the scattering vector. The elastic scattering is therefore strongest when $\boldsymbol{\kappa} = \boldsymbol{\tau}$ is perpendicular to the magnetization. On the other hand, the inelastic scattering is strongest when the scattering vector $\boldsymbol{\kappa} = \mathbf{q} + \boldsymbol{\tau}$ is along the magnetization, in which case, from (3.4.11),

$$\begin{aligned} \sum_{\alpha\beta} (\delta_{\alpha\beta} - \hat{\kappa}_\alpha \hat{\kappa}_\beta) \mathcal{S}^{\alpha\beta}(\boldsymbol{\kappa}, \omega) &= \frac{1}{\pi} \frac{1}{1 - e^{-\beta\hbar\omega}} \left(\chi''_{xx}(\mathbf{q}, \omega) + \chi''_{yy}(\mathbf{q}, \omega)\right) \\ &= \langle S_z \rangle \frac{1}{1 - e^{-\beta\hbar\omega}} \left\{\delta(\hbar\omega - E_{\mathbf{q}}) - \delta(\hbar\omega + E_{\mathbf{q}})\right\} \\ &= \langle S_z \rangle \left\{(n_{\mathbf{q}} + 1)\delta(\hbar\omega - E_{\mathbf{q}}) + n_{\mathbf{q}} \, \delta(\hbar\omega + E_{\mathbf{q}})\right\}, \end{aligned} \tag{4.2.11}$$

where $n_{\mathbf{q}} = (e^{\beta E_{\mathbf{q}}} - 1)^{-1}$ is the Bose population factor. The magnon-scattering intensity is thus proportional to the ordered moment, and the *stimulated emission and absorption* of the boson excitations, i.e. the magnons, due to the neutron beam, are proportional respectively to $(n_{\mathbf{q}} + 1)$ and $n_{\mathbf{q}}$, which may be compared with the equivalent result for light scattering from a gas of atoms.

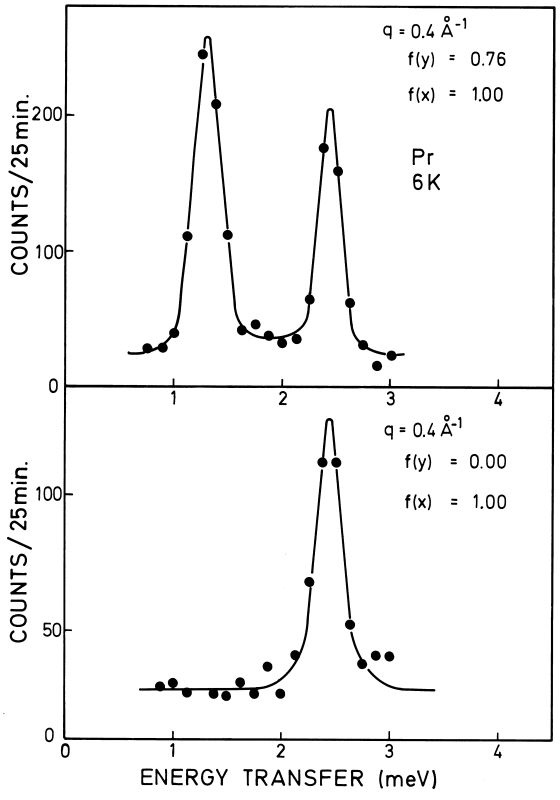

Fig. 4.2. A typical spectrum of inelastically-scattered neutrons in a constant-$\boldsymbol{\kappa}$ experiment, illustrating the determination of the dispersion relation and the polarization vector of the magnetic excitations. The peaks in the spectrum establish the energies of excitations which have a wave-vector $\mathbf{q}$, defined by the scattering vector through $\boldsymbol{\kappa} = \mathbf{q} + \boldsymbol{\tau}$, and thus determine points on the dispersion relation for Pr, shown in Fig. 7.1. The cross-section is proportional to the factor $f(\alpha) = 1 - (\kappa_\alpha/\kappa)^2$. Since $\mathbf{q}$ is along the ΓM (y)-axis, the absence of the peak of lower energy in the bottom figure shows unambiguously that it corresponds to a longitudinal mode.

The dependence of the intensity of inelastically scattered neutrons on the relative orientation of $\boldsymbol{\kappa}$ and the direction of the moment fluctuations is illustrated for the example of Pr in Fig. 4.2, which is discussed in more detail in Chapter 7. As in this figure, the scattering is normally measured as a function of $\hbar\omega$ at a fixed value of $\mathbf{q}$, a so-called *constant-*$\mathbf{q}$ or *constant-*$\boldsymbol{\kappa}$ *scan*, but occasionally *constant-energy scans*

may also be employed. In an actual experiment the directions and the lengths of $\mathbf{k}$ and $\mathbf{k}'$ are only defined with a limited degree of accuracy, and the δ-functions occurring in (4.2.10–11) are broadened into peaks with the shape of the *instrumental resolution function*, which to a good approximation is a Gaussian in the four-dimensional $(\boldsymbol{\kappa}, \omega)$-space. If the resolution function is known, it is possible to deconvolute the scattering peaks obtained in constant $\mathbf{q}$-scans from the broadening due to instrumental effects, and thereby determine the lifetimes of the excitations.

In this chapter, we have concentrated on the magnetic scattering of neutrons, but they may also be scattered through the interaction, via nuclear forces, with the nuclei in the sample. This interaction leads to a cross-section of the same order of magnitude as in the magnetic case, and it results in analogous phenomena to those discussed above, with the positions of the atoms replacing the magnetic moments as the fluctuating variables. The elastic Bragg scattering reveals the positions of the atoms in the crystal, and the elementary excitations appearing in the correlation functions are phonons. The fluctuations in the nuclear cross-section, due to the different spin states of the nuclei, give rise to an *incoherent* scattering, determined by the self-correlation of the individual atoms, in contrast to the *coherent* scattering, which is governed by the atomic pair-correlation function, in analogy with the magnetic scattering discussed above. Incoherence can also be produced by different isotopes of a particular element in a crystal, just as the variation of the magnetic moments in disordered alloys leads to incoherent magnetic scattering.

The magnetic scattering may be difficult to separate experimentally from the nuclear component. One possibility is to utilize the different temperature dependences of the two contributions, since the nuclear scattering normally changes relatively slowly with temperature. If this is not adequate, it may be necessary to perform *polarized* neutron scattering, in which the spin states of the incoming and scattered neutrons are determined, making it possible to isolate the scattering of purely magnetic origin (Moon, Riste and Koehler 1969). For further details of neutron scattering by nuclei in solids we refer to the texts mentioned at the beginning of this chapter.